Bifurcation study of azimuthal bulk flow in annular combustion systems with cylindrical symmetry breaking

Driek Rouwenhorst[1], Jakob Hermann[1] and Wolfgang Polifke[2]

Abstract

In annular combustion systems, azimuthal thermoacoustic modes manifest themselves predominantly as travelling or standing waves. Several phenomena can influence the modal behaviour of annular thermoacoustics. To monitor the stability of azimuthal thermoacoustics in industrial installations, a better understanding of the dynamics is required to correctly interpret online measurements. In this work, thermoacoustic eigensolutions of annular combustion systems are investigated, using a low-order analytic model. Heat release fluctuations are considered as a weak source term for a given acoustic eigenmode. The fluctuating heat release is modelled as a linear feedback to the local acoustics, in which the feedback response is a function of the azimuthal coordinate, causing cylindrical symmetry breaking. A bifurcation map is generated as a function of azimuthal mean flow velocity around the annulus. It is shown that a pitchfork bifurcation exists, separating standing wave and travelling wave solutions. Due to the interaction with non-uniform thermoacoustic feedback, an azimuthal flow with a low Mach number can significantly influence the system stability. Close to the bifurcation point, the non-normal nature of the dynamic system can induce a considerable gain of acoustic energy and yield more predictable time traces. These findings address the influence of non-normality, when applying a linear damping rate, acoustic amplitude or entropy-based quantity with the intent to monitor combustion dynamics in an annular combustion system.

1 Introduction

The risk of encountering a thermoacoustic instability in combustion systems increases under lean combustion conditions and a progressively variable power demand, as more renewable resources supply to the grid. A thorough understanding of the thermoacoustic feedback loop and the resulting measured dynamic signals is required for efficient control or monitoring strategies. In particular, the complex dynamics in annular gas turbines has not yet been fully understood. Complex conjugate wave pairs exist in the annulus as a result of the rotational symmetry, allowing for standing waves, travelling waves and combinations thereof. Fundamentally, the two azimuthal waves corresponding to an azimuthal mode number have repeated eigenvalues and form an eigenspace in linear stability analysis. Breaking of the cylindrical symmetry, either geometric or in the flame response, will typically lead to split eigenvalues. An example is a structural element in the annulus, causing reflections of azimuthal waves, leading to standing wave behaviour. Another example is single damaged burner with deviant feedback characteristics, which causes the standing wave in its orientation to have a different decay rate than the wave in orthogonal orientation. Considering the acoustics from the fixed coordinate system, an azimuthal flow also splits the eigenvalues, as the convection of the acoustic field causes a Doppler shift in the

[1]Research and Development, IfTA GmbH, Gröbenzell, Germany
[2]Department of Mechanical Engineering, Technische Universität München, München, Germany

Corresponding author:
Driek Rouwenhorst, IfTA Ingenieurbüro für Thermoakustik GmbH Industriestr. 33, Gröbenzell 82194, Germany.
Email: driek.rouwenhorst@ifta.com

frequency. Similar physics involving degenerate eigenvalue pairs are found in structural dynamics, such as eigenmodes in bladed disc assemblies. A study of Ewins shows the splitting of eigenmodes due to cylindrical symmetry breaking as a result of the mistuning of rotor blades.[1]

In this work, the interaction between azimuthal flow and cylindrical symmetry breaking is analysed analytically. The latter promotes standing wave behaviour as depicted before in the provided examples, whereas the former counteracts the formation of standing wave solutions by rotating the acoustic field with respect to the gas turbine. Upon commissioning of a gas turbine cylindrical symmetry cannot be guaranteed, because manufacturing margins and installation will for example cause some deviations in acoustic impedance from burner to burner. Wear, fouling and replacement of parts will add to the symmetry breaking. Regarding the azimuthal flow, no restriction is present in this direction. Azimuthal flow has been demonstrated both experimentally and numerically and is generally attributed to a co-swirling burner configuration. Wolf et al.[2] for example reports a bulk velocity exceeding an azimuthal Mach number of 1%, based on an extensive LES-simulation. Referring to the monitoring of combustion dynamics, it is of interest how the wave structures, amplitudes, decay rates and frequencies behave, when symmetry breaking and azimuthal flow are present simultaneously. The solution regimes (regarding standing and travelling wave structures) resulting from these effects have been recognized in Bauerheim et al.;[3] however, the interaction has not been investigated in detail. In the work of Noiray et al.,[4] the effect of nonlinear and non-uniform heat release response strength is investigated. The Fourier component C_{2n} of the non-uniformity was found to be responsible for the eigenvalue splitting. The effect of an azimuthal bulk flow was not considered.

The objective of the work is to investigate the transitional region between predominantly standing and travelling waves, in the parameter space spanned by symmetry breaking and azimuthal flow velocity. This is achieved by considering linear coupling between those phenomena in a low order description of the physical problem. The transition regime is characterized by a bifurcation, as a function of the relative strength of the two phenomena. The effect of non-normality of the linear system close to the bifurcation point is highlighted, as it turns out to have a significant influence on the statistical properties of the thermoacoustic amplitude under stochastic forcing. A small supplementary investigation is carried out to better understand the frequency split between clockwise (CW) and anticlockwise (ACW) acoustic waves. This phenomenon is often attributed to a mean flow around the annulus, that establishes when co-rotating swirl burners are used, but the details of this process are still unresolved.

The article consists of five sections, starting with this introduction. The next section treats the azimuthal flow and symmetry breaking in more detail, including the introduction of an effective source of azimuthal flow. The third section describes the modelling approach for the thermoacoustics, before the results are presented in 'Results: Feedback based on axial velocity' section. The final section concludes the work to be followed by references and three appendices with detailed derivations of used equations and the nomenclature.

2 Azimuthal flow and cylindrical symmetry breaking

In this section, the way the two phenomena, azimuthal flow and cylindrical symmetry breaking, can arise in annular combustion systems is explored. It is expected that effects causing symmetry breaking, including a non-uniform geometry and heat release response, cause split eigenvalues with standing wave eigenvectors. Azimuthal flow results in split eigenfrequencies for travelling wave eigenvectors, where it should be noted that the acoustic field is still degenerate in a coordinate system rotating with the mean flow.

A supplementary numerical investigation is carried out to understand the influence of a two-dimensional transverse velocity field. It demonstrates that a split in frequency of CW and ACW waves is not only related to a mean azimuthal velocity, but also to the gradient of azimuthal velocity with respect to the radial coordinate.

2.1 Azimuthal flow

In most annular combustion systems, flow around the annulus is not restricted in either the combustion chamber, or the plenum. In the axial direction, there is a constant flow of fresh and burnt gases that can reach high velocities at certain positions. It is to be expected that (depending on the operating conditions) some net momentum transfer in azimuthal direction occurs, for example, at the compressor exit in the plenum of the combustion chamber of a gas turbine or at the swirl burner in the combustion chamber. Experimental evidence of different acoustic propagation velocities in the opposing azimuthal directions can be found in Worth and Dawson[5] for varying burner separation distances. This has been wrongly attributed to a mean azimuthal flow alone,[2,5] as more than one phenomenon can be responsible for this split in frequencies.

The frequency splitting occurs when co-rotating swirl burners are used, however, co-rotating swirlers are expected to cause a velocity gradient, rather than
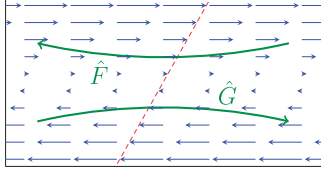
Figure 1. Refraction of acoustic waves in a velocity gradient. The direction of refraction depends on the direction of acoustic propagation and the refraction radius depends on the ratio of the velocity gradient and the speed of sound.
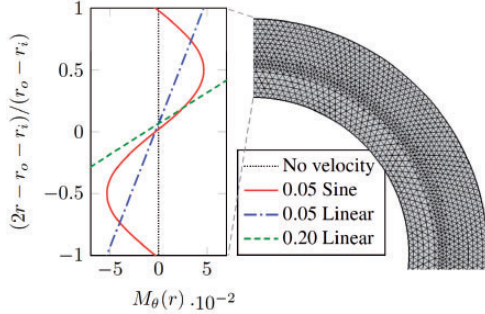

Figure 2. Tested azimuthal velocity profiles as a function of the radius. A quarter of the mesh used for the computation is shown on the right side.

Table 1. Increment of the eigenfrequencies as a result of azimuthal velocity gradients, with respect to frequency in the quiescent case ω_a. The first two mode orders m are given.

Velocity profile	m	$\omega_{cw}/\omega_a - 1$	$\omega_{acw}/\omega_a - 1$
No velocity	1	0	0
0.05 Sine	1	$-7.3 \cdot 10^{-3}$	$10.7 \cdot 10^{-3}$
0.05 Linear	1	$-8.6 \cdot 10^{-3}$	$11.0 \cdot 10^{-3}$
0.20 Linear	1	$-19.9 \cdot 10^{-3}$	$57.8 \cdot 10^{-3}$
No velocity	2	0	0
0.05 Sine	2	$-6.7 \cdot 10^{-3}$	$10.0 \cdot 10^{-3}$
0.05 Linear	2	$-8.0 \cdot 10^{-3}$	$10.2 \cdot 10^{-3}$
0.20 Linear	2	$-18.5 \cdot 10^{-3}$	$53.9 \cdot 10^{-3}$

a mean velocity. Therefore, it is investigated in this work whether a velocity gradient can also cause a split in the effective propagation speed between CW and ACW travelling waves. It is posed that a gradient of azimuthal velocity with respect to the radial coordinate, which refracts the acoustic waves as shown in Figure 1. A shear flow in an annulus refracts waves in one azimuthal direction towards the centre of the annulus. The wave in the other direction is constantly refracted towards the outer wall. A radially distributed azimuthal velocity field can be expected in annular combustion systems when co-rotating swirlers are used, refer to Bourgouin et al.[6] for a cold flow velocity field downstream of a swirl burner. Acoustic refraction can also be expected as a result of temperature gradients; however, this would affect the two waves in opposite direction identically, causing no split between the frequencies.

To demonstrate eigenvalue splitting as a result of a gradient of azimuthal velocity in the radial direction (refer to Figure 2), a 2D annular geometry with a ratio between the outer and inner radius of $r_o/r_i = 1.5$ is considered. Over the width of the annulus azimuthal velocity profiles are prescribed, without bulk flow contribution, as it would just add a known frequency split. A linear and harmonic profile with a peak to peak azimuthal Mach number of $M_{p2p} = 0.1$ is used. Additionally, a linear profile with a peak to peak of

$M_{p2p} = 0.4$ has been tested. The velocity in the latter case is too high to be expected in practice, but this case is used for analytical validation as the refraction radius is equal to the radius of the annulus. Acoustic solutions are obtained by solving the linear Euler equations numerically. COMSOL FEM software was used to obtain a solution in time domain, in which streamline diffusion was applied for stabilization. A quarter of the mesh is shown in Figure 2, together with the three prescribed velocity profiles. It must be noted that the velocity profiles include a small offset, in order to force the mean flow (integrated over the radial coordinate) to be zero.

The influence of the velocity profiles on the eigenfrequencies of azimuthal orders $m = 1$ and $m = 2$ are given in Table 1. The eigenfrequencies ω_{cw} and ω_{acw} correspond to a CW and an ACW travelling wave, respectively. It is concluded that waves that are refracted towards the centre of the annulus (which are CW waves for the used profiles in Figure 2), experience a decreased frequency. This can be explained by a loss of the radial wave number. When the refraction radius is equal to the radius of the annulus, plane wave propagation is obtained (in polar coordinates), with the lowest possible frequency, as the radial wave number is zero. The waves refracted away from the centre have an increased frequency. The lower frequency of the 0.20 linear velocity profile corresponds to the plane wave propagation in the polar coordinate frame, which is used for validation of the results. The theoretical frequency for this plane wave, normalized by the analytical solution without flow (quiescent solution, available in terms of Bessel functions), yields $\omega_{cw}/\omega_a - 1 = -19.7 \cdot 10^{-3}$. Table 1 shows that the theoretically and numerically found results deviate with 1% and 6%, for mode order 1 and 2, respectively. As this investigation is merely meant to demonstrate the existence and the order of magnitude of this phenomenon, such deviations are considered acceptable.

For $m = 1$ and a peak to peak azimuthal Mach number of $M_{p2p} = 0.1$, a difference in frequency of almost $0.02\omega_1$ is observed, which can be translated to an 'effective azimuthal Mach number' of $M_\theta \approx 0.01$. This investigation shows that a velocity gradient in the azimuthal flow can cause a significant split in wave propagation speed between the two directions. Despite this result, all possible effects that cause an apparent azimuthal bulk flow are represented by the angular bulk flow velocity v_θ in the remaining sections of this work, i.e. bulk flow is used as a paradigm for a split in the acoustic propagation velocity of opposing waves.

2.2 Cylindrical symmetry breaking

For fixed wavenumbers in the spatial directions, including a nonzero azimuthal mode order m, the acoustic field in an annulus is described by two complex amplitudes. A one-dimensional representation of azimuthal acoustics can be described by characteristic waves $\hat{F}$ and $\hat{G}$ for the ACW and CW acoustic propagation, respectively.

$$\hat{p}(\theta, t) = \hat{F}e^{i\omega_a t - im\theta} + \hat{G}e^{i\omega_a t + im\theta} \qquad (1)$$

When the pure travelling waves $\hat{F}$ and $\hat{G}$ have identical amplitudes, they form a standing wave around the circumference. In case of cylindrical symmetry (where geometry and parameters are invariant under angular rotation), the system manifests a pair of degenerate eigenvalues. Through non-uniformities in azimuthal direction the eigenvalues can split, i.e. lose the degeneracy. When the acoustic waves partially reflect at a certain angular location, the opposing waves couple and tend to form standing wave solutions. One could think of a slight constriction in azimuthal direction, caused by a structural element. The eigenvalues will be different for the standing waves with the structural element in the pressure node and the orthogonal wave with the element in the pressure antinode. A constriction mainly splits the eigenfrequencies,[7] but can also split the decay rate.

Similarly, acoustic sources (or sinks) varying with the azimuth can cause eigenvalue splitting. In particular, heat release fluctuations in response to acoustic perturbations form such an acoustic source. Examples of eigenvalue splitting through a non-uniform heat release response include retrofitting of burner parts at some location(s), designed to reduce the heat release response strength. When instability still occurs, it is most likely to develop perpendicular to the retrofitted burner(s). The alternating use of two burner types could be applied in an annular combustor (see the patent of Joos and Polifke[8]), in such a way that a smoother overall flame response that is less prone to

instabilities, is obtained. In such case, the chosen burner pattern influences the splitting strength and therefore the stability of the system, as pointed out by Berenbrink and Hoffman.[9]

Unintended azimuthal non-uniformities are likely to be present in industrial applications, for example, clogged fuel injection holes, deviations in acoustic impedance of the fuel injections and acoustic reflections from supporting structures. In this work, it is implied that the eigenvalue splitting is caused by a non-uniform flame response, but it might as well be of acoustic nature.

3 Modelling approach

The acoustics is described by a three-dimensional solution, satisfying the Helmholtz equation in an annulus, with two azimuthal wave amplitudes as free variables. The acoustic solution is convected passively with an azimuthal bulk flow. Axial flow is not considered, as it does not seem to influence the dynamic solution.[10] As in the work of Noiray et al.,[4] heat release fluctuations are continuously modelled over the azimuth of the annulus, rather than considering discrete burner locations. Local acoustic fluctuations result in heat release fluctuations at the corresponding angular location, through a linear flame response description. The heat release acts as a source to the acoustic pressure fluctuations, described on a Fourier basis over the azimuth.

A linear heat release response to acoustics perturbations is used, since the dynamic behaviour in the stable regime is sought, i.e. before exponential growth and saturation to a limit cycle occurs. It is assumed here that the magnitude of combustion noise does not cause a significant nonlinear response. Although saturation and limit cycle behaviour fall outside the scope of this work, initial growth rate and transient growth effects can still be studied in the unstable regime. Also, it is assumed that instantaneous growth rates and the angular bulk velocity are small compared to the considered eigenfrequency under all circumstances, such that time scales of amplitude modulations can be separated from the time scale of an acoustic cycle. This allows to average the equations over the acoustic cycles, resulting in compact analytic expressions. In this section, it will be shown that the resulting system of equations is a state space model with two complex degrees of freedom per degenerate acoustic eigensolution. The dynamic behaviour of this system is well suited for analytical evaluation.

3.1 Acoustic field

Thermoacoustics can be described by a sum of independent eigenmodes, based on solutions of the acoustic
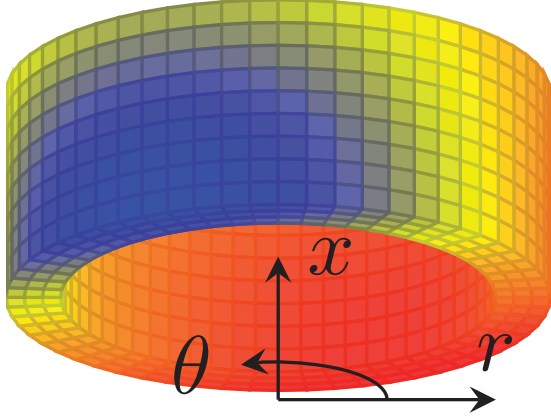
Figure 3. Example of an acoustic field of first azimuthal mode order, which could be described by equation (2).

field. Assuming that one modal solution of the 3D acoustic pressure field $\hat{p}$ with frequency ω_a is separable in the following way,

$$\hat{p}(\tilde{\mathbf{x}}, t) = \psi(x, r)\phi(\tilde{\theta})e^{i\omega_a t} \qquad (2)$$

The spatial function $\psi(x, r)$ is assumed to be known, fulfilling the wave equation for given longitudinal and radial boundary conditions in the annular combustion chamber. An example pressure field described by equation (2) is shown in Figure 3 for a generic annular geometry. Azimuthal dependency $\phi(\tilde{\theta})$ is not fully determined, as the periodic boundary condition merely enforces a continuous solution around the circumference.

$$\phi(\tilde{\theta}) = \hat{F}e^{-im\tilde{\theta}} + \hat{G}e^{im\tilde{\theta}} = \mathbf{b}^T\mathbf{z} \qquad (3)$$

In equation (3), the vector $\mathbf{z} = [\hat{F} \quad \hat{G}]^T$ contains the two Riemann invariants as free acoustic parameters, while $\mathbf{b} = [e^{-im\tilde{\theta}} \quad e^{im\tilde{\theta}}]^T$ contains their respective azimuthal basis functions. These basis functions satisfy the periodic boundary condition for a domain with uniform acoustic properties in the azimuthal direction for a positive definite azimuthal mode number m. The azimuthal coordinate $\tilde{\theta}$ is defined relative to the angular rotation $v_\theta t$, since the acoustics are passively convected by the flow field. In the fixed coordinate system of the combustor, the acoustics is obtained by substitution of $\tilde{\theta} = \theta - v_\theta t$.

Equation (2) is the fundamental solution of a 3D acoustic field in a cylindrically symmetric geometry with azimuthal bulk flow. Choosing the amplitudes $\hat{F}$ and $\hat{G}$, standing, travelling and mixed solutions can be constructed. The two amplitudes and complex angles

give four free variables, explaining the variety of possible wave structures.

The slow evolution of the acoustic amplitudes $\hat{F}$ and $\hat{G}$, as a result of global acoustic damping ζ and thermoacoustic feedback, is governed by equations (4).

$$\begin{aligned} \frac{\mathrm{d}}{\mathrm{d}t}\hat{F} &= -\zeta\omega_a\hat{F} + \kappa \oint \dot{Q}(\hat{F}, \hat{G})\hat{F}\mathrm{d}\theta \\ \frac{\mathrm{d}}{\mathrm{d}t}\hat{G} &= -\zeta\omega_a\hat{G} + \kappa \oint \dot{Q}(\hat{F}, \hat{G})\hat{G}\mathrm{d}\theta \end{aligned} \qquad (4)$$

The damping ratio is assumed to be small ($\zeta \ll 1$), such that the time scale of natural decay is long compared to the eigenfrequency. For brevity, the global damping ζ is ignored in this work, because it only superimposes on the eigenvalues of the thermoacoustic system. Heat release fluctuations $\dot{Q}$ are excited by the acoustics and form a source term in the acoustic equations, which is discussed in the following subsection. The proportionality constant κ is related to the volume of the acoustic domain and the ratio of specific heats.

3.2 Thermoacoustic feedback

Weak thermoacoustic feedback is added to the acoustic mode to find the combined dynamics. The thermoacoustic feedback is considered as small linear perturbations to the acoustic field, which justifies the performed separation in equation (2) of the acoustic time scale and the time scale with which the azimuthal acoustic field ($\phi(\tilde{\theta})$) changes. Dynamics dominated by the time scale of the combustion, such as intrinsic thermoacoustic instability,[11] are not considered.

The Rayleigh criterion states that acoustic energy is generated when heat release fluctuations $\dot{Q}$ are in phase with the pressure fluctuations. The growth of the acoustic mode in consideration is obtained by integrating over the volume in which the heat is released. Using $\star$ to denote the complex conjugate, the following equation can be derived (see Appendix 1).

$$\frac{\mathrm{d}\mathbf{z}}{\mathrm{d}t} = \kappa \oint \mathbf{b}^\star \dot{Q}\mathrm{d}\theta - v_\theta\left(\mathbf{b}^\star \cdot \mathbf{z} \cdot \frac{\mathrm{d}\mathbf{b}}{\mathrm{d}\tilde{\theta}}\right) \qquad (5)$$

This equation describes the time derivative of the two acoustic amplitudes in $\mathbf{z}$, resulting from the fluctuating heat release and an angular velocity. Prevailing methods for the modelling of heat release fluctuations assume a linear response to the acoustics at the burners, for low perturbation amplitudes. Examples are the flame transfer function and the sensitive time lag model.[12] Considering the response at the acoustic eigenfrequency ω_a only, these methods are in essence

identical. A general linear heat release response to the two acoustic waves can be written as

$$\kappa \dot{Q}(\theta) = \mathbf{b}^T \left(\begin{bmatrix} \hat{C}^F(\theta) & \hat{C}^G(\theta) \end{bmatrix}^T \cdot \mathbf{z} \right) \tag{6}$$

in which the complex-valued coefficients $\hat{C}^F$ and $\hat{C}^G$ represent the amplitude and phase of the heat release response to the respective waves in $\mathbf{z}$. These response coefficients are a function of the azimuth in case of non-uniform heat release, causing cylindrical symmetry breaking. Apart from the heat release, the coefficients can also include acoustic effects, such as attenuation and reflections. Combining the linear heat release response in equation (6) with the acoustic modal growth equation (5) yields a thermoacoustic system of ordinary differential equations.

$$\frac{d\mathbf{z}}{dt} = \oint \begin{bmatrix} \hat{C}^F + imv_\theta & \hat{C}^G e^{2im\theta} \\ \hat{C}^F e^{-2im\theta} & \hat{C}^G - imv_\theta \end{bmatrix} d\theta \, \mathbf{z} \tag{7}$$

From the integration of the system matrix over the azimuthal coordinate, it can be directly deduced that the diagonal only depends on the average of $\hat{C}^F$ and $\hat{C}^G$. On the other hand, the antidiagonal is only sensitive to coefficient $2m$ of the azimuthal Fourier decomposition of $\hat{C}^F$ and $\hat{C}^G$. This can be verified by recognizing that an integral of the form $\oint \exp(ik\theta)d\theta$ is zero for any nonzero integer k, because of the orthogonality of harmonic functions with different amounts of integer periods. Describing the coupling coefficients $\hat{C}$ as Fourier series over the azimuth allows the integration to be performed directly, by inserting the Fourier component that eliminates the harmonic dependency with respect to the azimuthal coordinate.

$$\hat{C}(\theta) = \sum_{k=-\infty}^{\infty} \hat{c}_k e^{ik\theta} \tag{8}$$

The coefficient $\hat{c}_0$ corresponds to the mean thermoacoustic feedback strength that influences the overall thermoacoustic stability. Equal to the C_{2n} coefficient in the work of Noiray et al.,[4] $\hat{c}_{2m}$ causes the eigenvalue pair of azimuthal mode order m to split. In this work, the coefficient is merely scaled differently, and it is complex, to cover heat release non-uniformities in both strength and phase. Physically, this means that standing wave eigenvalue splitting of a mode with azimuthal order m is only expected when the broken cylindrical symmetry has a non-zero Fourier component $2m$ around the circumference.

The azimuthal description of the thermoacoustic dynamics reduces to a complex second-order system of ODE's per azimuthal mode order. In Bauerheim et al.,[3] this solution structure was also found, modelling the heat release with an $n - \tau$ model.

$$\frac{d\mathbf{z}}{dt} = \begin{bmatrix} \hat{c}_0^F + imv_\theta & \hat{c}_{-2m}^G \\ \hat{c}_{2m}^F & \hat{c}_0^G - imv_\theta \end{bmatrix} \mathbf{z} \tag{9}$$

The coupling coefficients $\hat{c}_k$ can be a function of the frequency to be solved for, for example in the case of an $n - \tau$ model, where the phase linearly decreases with frequency.

$$\dot{\mathbf{z}} = M(\omega)\mathbf{z} \tag{10}$$

The system matrix M describes the coupling between the two (complex) acoustic degrees of freedom, including thermoacoustic interaction. Under additional flame response assumptions, the coupling coefficients can be specified in more detail, as demonstrated in Rouwenhorst et al.[13] for an $n - \tau$ flame model.

3.3 Solution strategy

The eigenvalues $\lambda_{1,2}$ of M prescribe the temporal evolution of the amplitude of the eigensolutions with multiplier $\exp(\lambda_{1,2}t)$. The real part of the eigenvalues describes the growth rate, of which the sign determines the stability of the mode. The imaginary part causes a frequency deviation with respect to the acoustic eigenfrequency ω_a.

In order to come to an analytic eigensolution of the system in equation (10), the system matrix must be independent of the frequency. When this is not the case, the characteristic equation of M(ω) is a transcendent equation for the eigenvalues (or complex frequency) that must be solved numerically. For small frequency dependency, however, using constant coupling values belonging to the frequency ω_a will yield accurate solutions.

The imaginary part of an eigenvalue of the system matrix M represents the frequency deviation $\Delta\omega$ from the acoustic eigenfrequency ω_a. When the coefficients $\hat{C}(\omega)$ are smooth and hardly change on the interval $[\omega_a - \Delta\omega < \omega < \omega_a + \Delta\omega]$, the frequency dependency can be neglected.

$$\left| \frac{\Delta\omega}{\hat{C}} \frac{d\hat{C}}{d\omega} \right|_{\omega_a} \ll 1 \tag{11}$$

As $\Delta\omega$ is of the order of $|\hat{C}|$, it can be stated that the derivative of the coupling parameters with respect to the frequency should be much smaller than one. Hence, the condition $d\hat{C}/d\omega \ll 1$ should be fulfilled at

the acoustic eigenfrequency in order to study the analytical solutions.

4 Results: Feedback based on axial velocity

In this section, further simplifications and assumptions are made in order to come to compact analytical expressions that enable to present the interaction between symmetry breaking and azimuthal bulk flow. Heat release fluctuations, due to vortical structures and equivalence ratio modulations, are usually attributed to the axial particle velocity (see Paschereit et al.,[14] for example). When axial particle velocity is held responsible for the fluctuating heat release, the thermoacoustic system is a function of the pressure fluctuations and independent of the azimuthal particle velocity. Assuming also that the coupling constants are (locally) independent of the frequency ($d\hat{C}/d\omega = 0$), the coupling parameters are identical ($\hat{C}^F = \hat{C}^G = \hat{C}$). These assumptions are made only to obtain a compact analytic eigensolution.

$$\frac{d\mathbf{z}}{dt} = \begin{bmatrix} \hat{c}_0 + imv_\theta & \hat{c}_{-2m} \\ \hat{c}_{2m} & \hat{c}_0 - imv_\theta \end{bmatrix} \mathbf{z} \qquad (12)$$

This system of differential equations, a function of mv_θ and the Fourier components of $\hat{C}(\theta)$, is used as the starting point of the analytic parameter study performed in this work. The eigensolution found is:

$$\lambda_{1,2} = \hat{c}_0 \pm \sqrt{\hat{c}_{2m}\hat{c}_{-2m} - m^2 v_\theta^2} \qquad (13)$$

In equation (13), it is visible how azimuthally varying heat release characteristics and azimuthal velocity split the eigenvalues $\lambda_{1,2}$ of the thermoacoustic system. The ratios of $\hat{F}$ and $\hat{G}$ corresponding to the eigenvectors, named $v_{1,2}$, are also readily obtained.

$$v_{1,2} = \frac{imv_\theta}{\hat{c}_{2m}} \pm \frac{1}{\hat{c}_{2m}}\sqrt{\hat{c}_{2m}\hat{c}_{-2m} - m^2 v_\theta^2} \qquad (14)$$

The influence of the model parameters on the acoustic eigensolution and their interaction will now be explained in detail. From the eigensolution, it can be seen that the interacting parameter groups are mv_θ, i.e. azimuthal velocity with respect to the azimuthal wave length, and the cylindrical symmetry breaking strength S. As the azimuthal velocity with respect to the wave length, mv_θ is a good parameter for azimuthal velocity, equations (13) and (14) suggest that

$$S = \sqrt{\hat{c}_{2m}\hat{c}_{-2m}} \qquad (15)$$

is a proper candidate to define as the symmetry breaking strength.

4.1 Uniform feedback $\hat{c}_0$ only ($mv_\theta = S = 0$)

This case corresponds to a setup with perfect cylindrical symmetry under quiescent conditions, i.e. no azimuthal flow. Without azimuthal non-uniformity of the thermoacoustic feedback response and no bulk velocity, the eigenvalues of the system are simply given by the constant feedback strength $\hat{c}_0$ on the diagonal of the system matrix. With repeated eigenvalues, the system is degenerate (i.e. solutions are defined by the eigenspace spanned by $\hat{F}$ and $\hat{G}$). This means that any linear combination of the two waves is an eigensolution, covering standing, travelling and mixed modes. The growth rate and frequency difference as a function of $\arg(\hat{c}_0)$ are the cosine and sine function, respectively.

4.2 Azimuthal flow mv_θ, with $S = 0$

This case corresponds to the theoretical setup with perfect cylindrical symmetry but now with an azimuthal flow through the annulus. Considering only azimuthal bulk flow, the same degenerate solution is found, now rotating with the mean flow. The rotation is visible in the imaginary split eigenvalues by $\pm imv_\theta$ for $\hat{F}$ and $\hat{G}$, respectively, in equation (13).

4.3 Cylindrical symmetry breaking S, with $mv_\theta = 0$

This case corresponds to a setup with quiescent flow conditions, but with a broken cylindrical symmetry that causes S to be non-zero. The symmetry breaking can be caused either by reflections (e.g. structural element) or a non-homogeniety in heat release response (e.g. clogged gas orifice in a burner). A pair of standing waves evolves as a result of the symmetry breaking, with eigenvalues that are split by S, as defined in equation (15). When S has a real contribution, a saddle point is formed by two orthogonal standing waves, one with positive and one with negative feedback. It can be understood that the azimuthal order $2m$ of $\hat{C}(\theta)$ causes this splitting, as it excites the $2m$ antinodes of these standing waves, respectively. In Figure 4, the growth rate and frequency are shown as a function of $\arg(S)$, which is the phase between the acoustic pressure and heat release rate. This phase is directly related to the phase of a flame transfer function, which is often used to describe the heat release response to acoustic excitation.

4.4 Interaction between mv_θ and S

This case corresponds to the general situation in practical systems, where azimuthal velocity and symmetry breaking are expected to coexist. As both mv_θ and S appear in the root in the eigensolution equations (13) and (14), some interaction takes place, shaping the
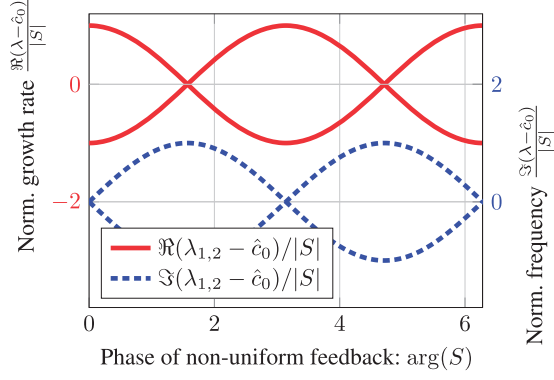
Figure 4. Effect of the phase of the non-uniform feedback $\arg(S)$ on the eigenvalues of the thermoacoustic system, without angular bulk velocity v_θ. Normalization by the cylindrical asymmetry strength $|S|$.

Figure 5. Normalized effect of the interaction between mv_θ and cylindrical symmetry breaking S on the eigenvalues of the thermoacoustic system, with $\arg(S) = 0$. In gray thin lines, the result for $\arg(S) = \pi/6$.

modal solutions. What the eigenmodes look like is not directly clear from the analytic expressions. The interaction in this intermediate regime can be understood qualitatively as follows; the azimuthal feedback non-uniformity tries to develop a standing wave solution, but the bulk velocity constantly rotates the acoustic field away from its standing wave angle. Two new equilibria will therefore evolve, given by the full eigensolution. The interaction is most pronounced when the two effects are of similar magnitude; $|S| \approx |mv_\theta|$. In the regime where $|mv_\theta/S| \ll 1$, solutions are predominantly standing waves, whereas $|mv_\theta/S| \gg 1$ is better characterized as travelling waves.

The velocity term can cancel out the eigenvalue splitting as a result of the symmetry breaking strength. An important observation is that only limited azimuthal velocity is required for noticeable changes in the stability analysis. Instability is most likely to occur in strongly underdamped (thermo)acoustic eigenmodes, say with a damping ratio of the order $\zeta = \mathcal{O}(10^{-2})$. Azimuthal velocity can potentially change the stability with strength mv_θ, therefore azimuthal Mach numbers of the same order $M_\theta = \mathcal{O}(10^{-2})$ are already relevant in the presence of cylindrical symmetry breaking.

4.5 Bifurcation point

The case where $\hat{c}_{2m} = \hat{c}_{-2m}^\star$ is of most interest, because the feedback contributes optimally to the real part of the eigenvalues and thus to the system stability. Physically, this occurs when the non-uniform part of the feedback response $\hat{C}(\theta)$ is real, i.e. the non-uniform heat release response acts in phase with acoustic pressure oscillations. The symmetry breaking S is real and the feedback phase is constant around the azimuth. The bifurcation diagram with mv_θ as the bifurcation parameter forms a unit circle and unit parabola for the growth
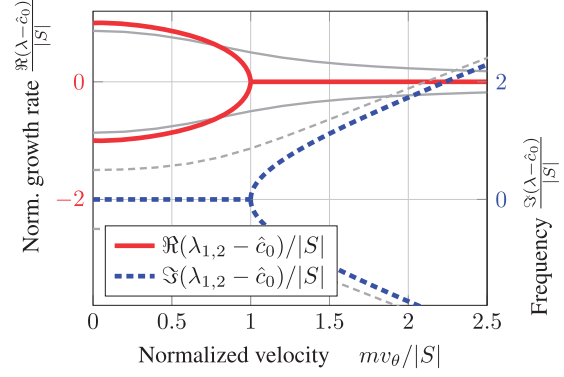
rate and frequency difference, respectively, when normalized by $|S|$ (see Figure 5). Without azimuthal velocity, two standing wave solutions in orthogonal orientations are found, with pure positive and negative feedback. In a phase portrait, this solution is represented by a saddle point (shown in Figure 6(a)). As a mean flow is introduced, the splitting of the growth rate decreases and simultaneously the eigenvectors lose their mutual orthogonality. A bifurcation point at $|mv_\theta| = S$ emerges as the discriminant in the root of the dynamical solutions crosses zero. At this point, the two eigenvectors coincide, as Figure 6(e) suggests. In other words, the eigenvectors are linearly dependent and the system matrix is defective. For comparison, a case with complex S is shown in Figure 5 (thin gray lines) that does not cross the bifurcation point. In that case, the feedback partially acts on the frequency, preventing the discriminant in the eigensolution (equations (13) and (14)) to become zero.

The bifurcation point as shown in Figure 5 can be dangerous during the operation of an annular combustion system. As the bifurcation parameter varies a little, the stability can abruptly change near the bifurcation point.

4.6 Non-normal growth

In the case of non-normality, especially, coinciding eigenvectors, perturbations to the system can experience transient amplification. When the system has a nonlinear response to the amplitude, an instability can be triggered even though the system is fixed point stable at zero amplitude. Non-normal growth has been studied in thermoacoustic systems, based on modelling[15] as well as experiments.[16] In this section, non-normal growth in annular combustion systems is demonstrated in the bifurcation point of the model
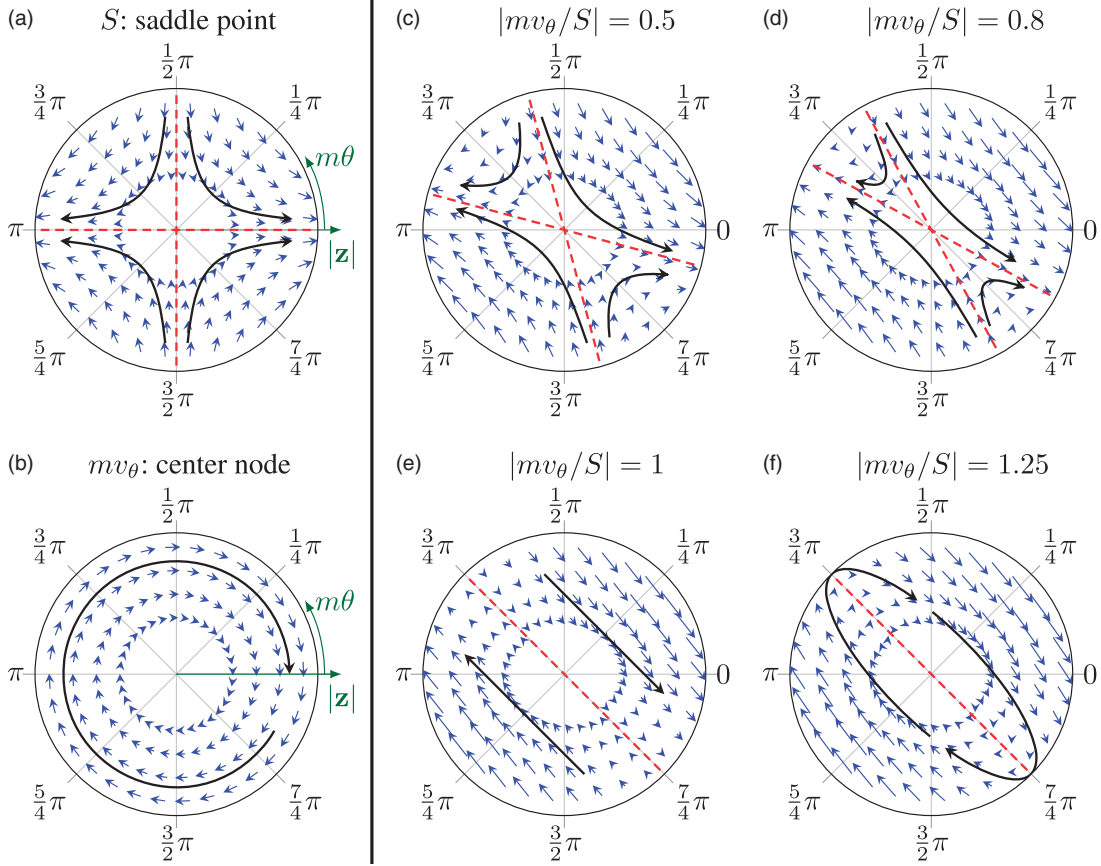
Figure 6. Phase portraits of the thermoacoustic system for real azimuthal symmetry breaking S, in the vector space of two orthogonal standing waves. Vectors show the tangents of possible dynamic trajectories, of which a few options are plotted by curved arrows. Eigenvectors are shown as dashed lines passing through the origin. The acoustic amplitude $|z(t)|$ is represented by the radial distance to the origin and the angular orientation $m\theta$ of the standing wave can be read from the angle in the phase portrait. (a) A real azimuthal asymmetry S results in a saddle point, with an unstable standing wave with orientation $m\theta = 0$ and a stable standing wave at $m\theta = \pi/2$. (c,d) Increasingly adding azimuthal velocity – a centre node shown in (b) – brings the eigenvectors together. In the bifurcation point (e), a neutrally stable improper node is found, with coinciding eigenvectors. (f) For higher velocities, the standing wave solutions are convected by the flow, rather than being kept in place by the cylindrical symmetry breaking. A contribution of $\hat{c}_0$ could be included by superposing a star node, influencing the overall stability.

system. Due to the annular geometry, the amplitude amplification can occur at a single mode order revealing an insightful physical mechanism behind the transient growth.

The dynamic solution of the defective system matrix takes the form

$$\mathbf{z}(t) = 2S\left(Ate^{\hat{c}_0 t} + Be^{\hat{c}_0 t}\right)\mathbf{v} + Ae^{\hat{c}_0 t}\mathbf{w} \qquad (16)$$

where $\mathbf{v}$ is the (repeated) eigenvector, while $\mathbf{w}$ is chosen as the standing wave orthogonal to $\mathbf{v}$. Amplitudes A and B follow from initial conditions.

The term $Ate^{\hat{c}_0 t}$ causes the transient behaviour before the exponential decay sets in. Transient growth can occur only when the system would have been unstable in one orientation (saddle point), if there were no azimuthal bulk flow. From the solution in

equation (16), the maximum transient growth can be obtained analytically (see Appendix 2). For $\Re(\hat{c}_0)^2 \ll S^2$, the time after which the maximum amplification occurs is approximately $t_{\max} = -1/\Re(\hat{c}_0)$. At this point, a maximum possible amplification ratio is reached of about

$$\frac{|\mathbf{z}(t)|}{|\mathbf{z}_0|} = \frac{-2S}{\Re(\hat{c}_0)e} \qquad (17)$$

The transient growth is demonstrated for $S = mv_\theta = 10s^{-1}$ and a thermoacoustic decay of $\Re(\hat{c}_0) = -2s^{-1}$. The phase portrait of the dynamic system is shown in the top of Figure 7. The two thick lines represent the solutions that experience the maximum possible transient growth, starting on the unit circle. In the plot below this transient growth of the
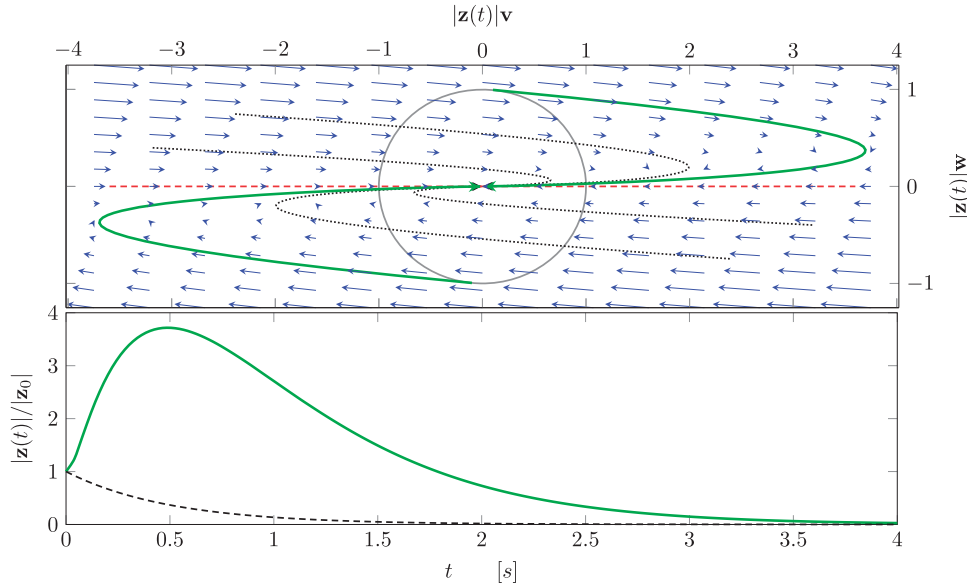
Figure 7. Transient growth of the acoustic amplitude in the bifurcation point of the system, with $S = mv_\theta = 10s^{-1}$ and $\lambda = \Re(\hat{c}_0) = -2s^{-1}$, starting from the initial conditions that lead to the maximum transient growth. Above, the evolution in the phase portrait (eigenvector aligned with the x-axis) shows the rotation of the acoustic field. Below, the growth is plotted as a function of time, compared to the case of normal decay (dashed line). The maximum growth amplification is accurately approximated by equation (17).

amplitude is shown as a function of time. A maximum amplitude amplification of 3.7 is reached as estimated by equation (17). This is equivalent to an amplification factor of over 13 for the acoustic energy.

Alternatively, the maximum amplification and the corresponding initial conditions can be found computationally (see for example Nagaraja et al.[17]). Using this approach, the same results have been found (not shown). For this specific low-order model, the amplification can be computed analytically at the bifurcation point. In this way, it has been found theoretically that infinite transient growth can be obtained for nonzero splitting strength and vanishing stability (refer to case $|mv_\theta/S| = 1$ in Figure 6(e), where a perturbation away from the eigenvector pair linearly grows to infinity, even though the system is marginally stable).

With help of the phase portrait representations, the transient behaviour of this system can be easily understood physically. A perturbation in an unstable orientation of the symmetry breaking will initialize exponential growth. In the phase portrait of Figure 7, these orientations are located in quadrant 1 (positive–positive) and quadrant 3 (negative–negative). The azimuthal flow then convects the growing amplitude around the circumference towards the stable orientation of the saddle node. The growth will eventually come to a halt and the perturbation will converge to the least stable eigenmode and decay accordingly.

4.7 Amplitude statistics under stochastic excitation

The maximum transient amplification shows what amplitude can be reached for an optimized initial condition. More interesting is what effect the non-normality of the system has on the characteristics under constant stochastic forcing. To investigate this, the system of equations (equation (12)) has been integrated numerically with white noise excitation, using the Euler–Mayurama scheme. The system is compared to the uncoupled, degenerate case (uniform heat release response) with the same set of eigenvalues $\Re(\lambda_{1,2}) = \Re(\hat{c}_0) = -2s^{-1}$. Part of the two time series that were subjected to the same excitation noise are shown in Figure 8. The average amplitude (RMS) of the non-normal system is found to be 5 times higher (25 times for the acoustic energy) than the degenerate system, which is higher than the maximum possible non-normal growth ratio. This result suggests it is more interesting to look at the integral of the amplitude over time for all initial conditions, rather than looking at the maximum possible amplification.

The probability density function of the Euclidean norm of four independent, normal distributed variables (two complex amplitudes) is given by the χ_4 distribution. The histogram of the bottom time series in Figure 8 shows that the χ_4 distribution accurately describes the probability of the amplitudes found for the uncoupled thermoacoustic system. For the
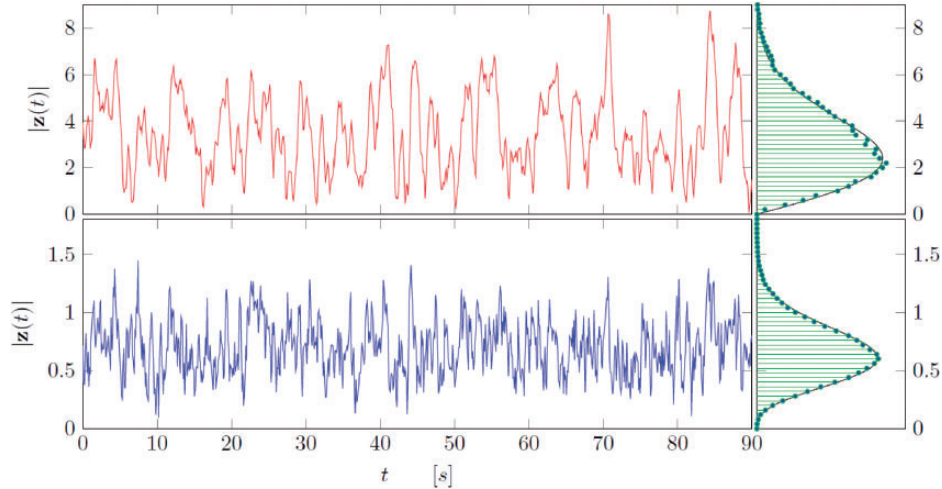
Figure 8. Time series of stochastically forced systems, with eigenvalues $\lambda_{12} = -2s^{-1}$. Above: bifurcation point; below: degenerate case (uncoupled). The RMS value of the non-normal system is 5 times higher compared to the degenerate case, both under unit forcing strength. Note the difference in amplitude histograms (based on 14 min) on the right, compared to χ_2 and χ_4 distributions (solid lines), respectively.

non-normal system matrix, however, the amplitude distribution is much better described by the χ_2 distribution, i.e. a process with only two independent variables. This result can be explained by the strong coupling of the waves (caused by the anti-diagonal in the system matrix, equation (12)), predominantly yielding standing waves under a preferred angular orientation. The latter distribution has a higher kurtosis than the former, which means that the observed peaks in the time series are relatively high with respect to the mean amplitude.

When monitoring a stochastically forced oscillating signal, the exponential decay of the autocorrelation function can normally be used to estimate the damping of the system.[18] Underlying assumption is that the oscillation comes from a dynamic system that can be described by a single damped harmonic oscillator. In the annular geometry, the dynamics is described by two coupled harmonic oscillators, which is why the damping cannot be obtained from the autocorrelation decay. Especially in this example with a strong non-normal system matrix, the autocorrelation function does not show a clear behaviour of exponential decay and the decay is much slower than expected from the eigenvalue pair. Moreover, this example shows that monitoring strategies that are meant to warn for unstable combustion dynamics, respond differently to the non-normal nature of the system, depending on the monitored quantity. Stability criteria based on acoustic amplitude and the entropy of the signal (see for example Sarkar et al.[19]) would indicate a significantly reduced stability margin for the non-normal system, compared to the normal system with identical damping rate.

5 Conclusions

An annular thermoacoustic system with both azimuthal bulk flow and non-uniform response can show highly interesting dynamics, even under linear assumptions. As the damping ratio is typically much smaller than one, it is found that small azimuthal Mach numbers can be relevant for the thermoacoustic stability through the interaction with azimuthal non-uniformities. Similar to the C_{2n} criterion in Noiray et al.,[4] specific Fourier components of the non-uniform heat release in the annulus are found to contribute to eigenvalue splitting, resulting in two orthogonal standing wave solutions. A concurrent split in the acoustic propagation velocity between CW and ACW waves, however, impairs the formation of standing wave solutions.

Solving the acoustic field numerically, it is demonstrated that a velocity gradient in the azimuthal flow, induced by co-rotating swirlers, cause a frequency split through the refraction of acoustic waves. This implies that a slowly rotating acoustic field does not prove the presence of an azimuthal bulk flow in the annulus. The split in frequency between ACW and AC waves is, against this new knowledge, conveniently expressed in terms of an effective azimuthal flow. The azimuthal flow can stabilize standing wave solutions that would otherwise be unstable as a result of a broken geometrical symmetry or non-homogeneous flame response. In reverse, a loss of azimuthal flow can cause a sudden decrease of thermoacoustic stability. As the effective azimuthal flow follows from operating conditions in a non-trivial way, instability can occur unexpectedly. Therefore, the coupling between the acoustic field and the azimuthal flow

field could be an important nonlinear phenomenon in thermoacoustics of annular gas turbines.

The type of eigenmode solution depends on the ratio between the azimuthal flow velocity per wavelength and the cylindrical asymmetry. When their strengths are of the same order of magnitude, both phenomena must be regarded in the stability analysis of annular thermoacoustic systems. When the ratio is close to one, the system can behave in a strongly non-normal manner. A bifurcation point exists where the system matrix is defective. It is shown analytically that the maximum transient growth in this point is infinite for vanishing system stability. This prove of transient growth for azimuthal modes, considering just a single mode order, comes with a comprehensible physical explanation; an azimuthal velocity rotates an acoustic field past angular orientations with varying instantaneous growth rates, modulating the amplitude transiently.

A non-normal system can yield significantly higher amplitudes when stochastic forcing is applied, compared to the degenerate counterpart with equal eigenvalues. This effective amplification under random excitation is considered more relevant than the maximum possible transient amplification ratio. The statistical moments of the acoustic amplitude also change as a result of the linear coupling between the waves. The increased peakedness of the amplitude should not be mistaken with intermittency due to nonlinearities. For the monitoring of combustion dynamics (such as amplitude, decay rate and instability precursors), it is valuable to know that azimuthal eigenmode pairs can behave non-normal and how typical monitoring quantities respond to this. It is shown that for constant damping rate (i.e. thermoacoustic stability), the acoustic amplitude and predictability of the time series can rise remarkably for increased non-normality.

Declaration of Conflicting Interests

The author(s) declared no potential conflicts of interest with respect to the research, authorship, and/or publication of this article.

References

1. Ewins DJ. Vibration characteristics of bladed disc assemblies. *J Mech Eng Sci* 1973; 15: 165–186.
2. Wolf P, Staffelbach G, Gicquel LYM, et al. Acoustic and Large Eddy Simulation studies of azimuthal modes in annular combustion chambers. *Combust Flame* 2012; 159: 3398–3413.
3. Bauerheim M, Salas P, Nicoud F, et al. Symmetry breaking of azimuthal thermo-acoustic modes in annular cavities: A theoretical study. *J Fluid Mech* 2014; 760: 431–465.
4. Noiray N, Bothien M and Schuermans B. Investigation of azimuthal staging concepts in annular gas turbines. *Combust Theory Modell* 2011; 15: 585–606.
5. Worth NA and Dawson JR. Modal dynamics of self-excited azimuthal instabilities in an annular combustion chamber. *Combust Flame* 2013; 160: 2476–2489.
6. Bourgouin JF, Durox D, Schuller T, et al. Ignition dynamics of an annular combustor equipped with multiple swirling injectors. *Combust Flame* 2013; 160: 1398–1413.
7. Choe SY. *Investigation of a constricted annular acoustic resonator*. Master Thesis, Naval Postgraduate School, http://calhoun.nps.edu/bitstream/handle/10945/8575/investigationofc00choe.pdf (1997, accessed 8 June 2017).
8. Joos F, Polifke W and Ni A. Combustion device for generating hot gases, http://patft1.uspto.gov/netacgi/nph-Parser?patentnumber=6449951 (2002, accessed 8 June 2017).
9. Berenbrink P and Hoffmann S. Suppression of dynamic combustion instabilities by passive and active means. In: *International gas turbine and aeroengine congress & exposition*, 2000-GT-0079, ASME, Munich, pp.7–7.
10. Evesque S, Polifke W and Pankiewitz C. Spinning and azimuthally standing acoustic modes in annular combustors. In: *Proceedings of the 9th AIAA/CEAS aeroacoustics conference*, Paper AIAA 2003-3182, 12–14 May 2003, Hilton Head, South Carolina, AIAA 2003-3182, http://arc.aiaa.org/doi/pdf/10.2514/6.2003-3182 (2003, accessed 8 June 2017).
11. Emmert T, Bomberg S and Polifke W. Intrinsic thermoacoustic instability of premixed flames. *Combust Flame* 2015; 162: 75–85.
12. Crocco L and Cheng SI. *Theory of combustion instability in liquid propellant rocket motors*. London: Butterworths Science Publication, 1956, pp.021502-1–021502-8.
13. Rouwenhorst D, Hermann J and Polifke W. Online monitoring of thermoacoustic eigenmodes in annular combustion systems based on a state-space model. *J Eng Gas Turb Power* 2017; 139: 021502-1–021502-8.
14. Paschereit CO and Polifke W. Investigation of the thermoacoustic characteristics of a lean premixed gas turbine burner. In: *International gas turbine and aeroengine congress & exposition*, Stockholm, ASME 98-GT-582.
15. Juniper M. Triggering in the horizontal Rijke tube: Non-normality, transient growth and bypass transition. *J Fluid Mech* 2011; 667: 272–308.
16. Kim KT and Hochgreb S. Measurements of triggering and transient growth in a model lean-premixed gas turbine combustor. *Combust Flame* 2012; 159: 1215–1227.

17. Nagaraja S, Kedia K and Sujith RI. Characterizing energy growth during combustion instabilities: Singularvalues or eigenvalues? *Proc Combust Inst* 2009; 32: 2933–2940.

18. Lieuwen T. Online combustor stability margin assessment using dynamic pressure data. *Trans ASME* 2005; 127: 478–482.

19. Sarkar S, Chakravarthy SR, Ramanan V, et al. Dynamic data-driven prediction of instability in a swirl-stabilized combustor. *Int J Spray Combust Dyn* 2016; 8: 235–253.

Appendix 1

Derivation of equation (5): The Rayleigh criterion can be written as

$$\frac{1}{\gamma - 1}\frac{D}{Dt}(\hat{p}^\star \hat{p}) = \dot{Q}\hat{p}^\star + \dot{Q}^\star \hat{p} \tag{18}$$

Regarding the slow azimuthal dynamics

$$\frac{1}{\gamma - 1}\frac{D}{Dt}(\phi^\star \phi) = \dot{Q}\phi^\star + \dot{Q}^\star \phi \tag{19}$$

Seeking the complex growth of ϕ as a function of the heat release $\dot{Q}$, we can keep the following part

$$\phi^\star \frac{D\phi}{Dt} = (\gamma - 1)\dot{Q}\phi^\star \tag{20}$$

The equation has to hold for both amplitudes in $\mathbf{z}$ independently as the basis functions are orthogonal, so we can write

$$\frac{D\mathbf{b} \cdot \mathbf{z}}{Dt} = (\gamma - 1)\dot{Q} \tag{21}$$

writing out the total derivative

$$\mathbf{b} \cdot \frac{d\mathbf{z}}{dt} + v_\theta \left(\mathbf{z} \cdot \frac{d\mathbf{b}}{d\theta} \right) = (\gamma - 1)\dot{Q} \tag{22}$$

to retrieve the effect on $\mathbf{z}$

$$\frac{d\mathbf{z}}{dt} = (\gamma - 1)\mathbf{b}^\star \dot{Q} - v_\theta \left(\mathbf{b}^\star \cdot \mathbf{z} \cdot \frac{d\mathbf{b}}{d\tilde{\theta}} \right) \tag{23}$$

The average effect over the volume V can be written as

$$\frac{d\mathbf{z}}{dt} = (\gamma - 1)V \oint \mathbf{b}^\star \dot{Q}d\theta - v_\theta \left(\mathbf{b}^\star \cdot \mathbf{z} \cdot \frac{d\mathbf{b}}{d\tilde{\theta}} \right) \tag{24}$$

because the right-most term is not a function of θ. The volume and ratio of specific heats are combined in a single proportionality constant: $\kappa = (\gamma - 1)V$

$$\frac{d\mathbf{z}}{dt} = \kappa \oint \mathbf{b}^\star \dot{Q}d\theta - v_\theta \left(\mathbf{b}^\star \cdot \mathbf{z} \cdot \frac{d\mathbf{b}}{d\theta} \right) \tag{25}$$

Appendix 2

Derivation of equation (17): We have the solution in terms of two standing waves (equation (16))

$$\mathbf{z}(t) = 2S\left(Ate^{\hat{c}_0 t} + Be^{\hat{c}_0 t}\right)\mathbf{v} + Ae^{\hat{c}_0 t}\mathbf{w} \tag{26}$$

A solution that starts on a unit circle and reaches the maximum will start tangential to the unit circle and then grow. This means the first derivative of the acoustic energy is zero (and the second positive). The acoustic energy is

$$|\mathbf{z}^2(t)| = \left(4S^2(At + B)(A^\star t + B^\star) + AA^\star\right)e^{2\Re(\hat{c}_0)t} \tag{27}$$

We know that travelling waves decay with $-\Re\lambda$ without growing transiently (on a time scale longer than a cycle). Therefore, any travelling energy content would reduce the transient growth. For this reason, we reduce our search to real values for A and B. Derivative at $t = 0$, starting on the unit circle: $A^2 + 4S^2B^2 = 1$

$$|\mathbf{z}^2|'_{t=0} = 4ABS^2 + \Re(\hat{c}_0) = 0 \tag{28}$$

Solutions for A and B are

$$A = \pm\sqrt{\frac{1}{2} \pm \frac{1}{2}\sqrt{1 - \frac{\Re(\hat{c}_0)^2}{S}}} \tag{29}$$

$$B = \frac{\sqrt{1 - A^2}}{2S} = \pm\sqrt{\frac{1}{8S^2} \mp \frac{1}{8S^2}\sqrt{1 - \frac{\Re(\hat{c}_0)^2}{S^2}}} \tag{30}$$

One of the (positive and negative) solution pairs are the initial condition for maximum growth, whereas the other pair points to the conditions where the maximum amplitude is located. This can be deduced by looking at the second derivative of the acoustic energy. Inserting the found initial amplitudes in the derivative of acoustic energy, the time to the maximum amplitude can be solved for

$$\frac{1}{2}|\mathbf{z}^2(t)|'e^{-2\Re(\hat{c}_0)t}$$
$$= 4S^2(A^2 t(\Re(\hat{c}_0)t + 1) + AB(2\Re(\hat{c}_0)t + 1)) + \Re(\hat{c}_0) \tag{31}$$

Solving the polynomial for the time t, the time t_{max} is found at which the maximum amplitude is reached

$$t_{max} = \frac{-1}{\Re(\hat{c}_0)} \sqrt{1 - \frac{\Re(\hat{c}_0)^2}{S^2}} \qquad (32)$$

Backsubstitution of t_{max} and amplitudes A and B in equation (27) yield the maximum amplitude growth, given by

$$\left|\frac{\mathbf{z}}{\mathbf{z_0}}\right|_{max} = \frac{-\Re(\hat{c}_0)}{S} \frac{e^{-\sqrt{1 - \frac{\Re(\hat{c}_0)^2}{S^2}}}}{1 - \sqrt{1 - \frac{\Re(\hat{c}_0)^2}{S^2}}} \qquad (33)$$

Clearly for $S^2 = \hat{c}_{2m}\hat{c}_{-2m} \gg \Re(\hat{c}_0)^2$, this can be simplified to

$$\left|\frac{\mathbf{z}}{\mathbf{z_0}}\right|_{max} = \frac{-\Re(\hat{c}_0)}{eS} \frac{1}{\frac{\Re(\hat{c}_0)^2}{2S^2}} = \frac{-2S}{\Re(\hat{c}_0)e} \qquad (34)$$

Appendix 3

Nomenclature

A, B Acoustic amplitudes of the defective system

$\mathbf{b}$ Vector with acoustic amplitudes $\hat{F}$ and $\hat{G}$

$\hat{c}_k$ Fourier components of $\hat{C}(\theta)$

$\hat{C}(\theta)$ Azimuthal feedback strength distribution

$\hat{F}$ Anticlockwise travelling acoustic wave

$\hat{G}$ Clockwise travelling acoustic wave

m   Azimuthal mode order

M   Thermoacoustic system matrix

M Mach number

$\dot{Q}(\theta)$ Fluctuating heat release

S   Cylindrical symmetry breaking strength

v_θ Angular velocity

$\mathbf{v}, \mathbf{w}$ Standing wave vectors for the defective system

$\mathbf{z}$ Vector with azimuthal basis functions

ζ Natural acoustic damping

$\tilde{\theta}$ Moving azimuthal coordinate $(\theta - v_\theta t)$

κ Feedback proportionality constant

λ Eigenvalue of the thermoacoustic system

ν Eigenvector of the thermoacoustic system

$\phi(\theta)$ Acoustic field along the azimuthal coordinate

$\psi(x, r)$ Acoustic field along the axial and radial coordinates